

Measurement and optimization of nonlinear damping systems for agricultural engineering vehicle cab

Xin Zhang, Yuanyou Liu, Zhanlong Li, Zengliang Xiao

School of Mechanical Engineering, Taiyuan University of Science and Technology, China

Abstract

The issue of nonlinear dampness in the cab of agricultural engineering vehicles is examined by analyzing the vibration reduction system of a specific agricultural loader. Firstly, the specific loader was tested under different conditions. Then, the nonlinear vibration reduction system model of the cab-seat-human body is established by using the measured frame vibration signal as input. Finally, the multi-objective genetic algorithm is used to optimize the root mean square (RMS) value of vertical acceleration of the cab and seat. The test results show that the seat vibration is significantly greater than the acceleration of the cab floor under driving and working conditions, so the seat vibration is amplified and the seat parameter setting is unreasonable; the engine and the working device are also an important part of the cab vibration source, in addition to the uneven road surface. Comparing the RMS values of the vertical acceleration of the cab and seat, which were calculated by the model and obtained from

the vehicle test, the error does not exceed 6%, indicating that the model's accuracy meets the requirement. The vehicle experiment proves that the RMS value of the vertical acceleration of the cab and seat is reduced by 16% and 53%, respectively, after optimization. This study provides a theoretical basis for the design of the damping system for the cab of agricultural engineering vehicles.

Introduction

The agricultural engineering vehicles have a harsh working environment, and severe vibrations seriously affect the health of the driver. Therefore, the vibration of the cab has always been a major concern in the development of agricultural engineering vehicles (Li *et al.*, 2021; Nguyen *et al.*, 2020; Zhao *et al.*, 2020). The vibration sources in the cab of agricultural engineering vehicles are diverse, such as excitation from the ground during driving, excitation from working devices during operation, and excitation from the engine (Li *et al.*, 2017; Junji *et al.*, 2017; Palumbo *et al.*, 2021). Therefore, the design of the vibration reduction system for the cab of agricultural engineering vehicles should be able to meet the vibration reduction requirements under different conditions (Debeleac *et al.*, 2021; Stan *et al.*, 2015; Sun *et al.*, 2020). Currently, many scholars are studying the damping performance of the cab of agricultural engineering vehicles by establishing a whole vehicle vibration system model that includes tires, suspension, a suspended cab, and mounted seats. Using road roughness as input, they analyze and optimize the vibration reduction performance of the cab under different road conditions. As Lin *et al.* (2019) introduced a 15-degree-of-freedom vehicle model consisting of a cab, a compartment, a chassis, and suspension to present the vibration behavior of the vehicle cab. Tao *et al.* (2020) considered the vibration characteristics of the working device and the four-wheel-related random road excitation to establish a dynamic model of the agricultural engineering vehicle cab, and then improved the vibration reduction performance of the agricultural engineering vehicle cab through simulation analysis. Zeng (2011) used excitation analysis such as road surface and tire to prove that the walking stability system could improve the driving stability of the whole agricultural engineering vehicle and reduce the vibration of the cab. Jamali *et al.* (2014) developed a 5-degree-of-freedom cab model that could approximate vehicle performance by using simulations with actual random road power spectral density. They used multi-objective genetic algorithm optimization with the root mean square (RMS) value of seat acceleration as the target, which improved the vibration performance of the cab. Although such models have a wide range of applications, they differ significantly from the actual excitation that the cab damping system receives. Some scholars have also studied the resonance effect of engine excitation frequency on the cab structure, and improved the flexible cab structure accordingly. Liu *et al.* (2020) analyzed the vibration acceleration spectra of each measurement point and found that the vibration amplification problem of the cab was

Correspondence: Xin Zhang, School of Mechanical Engineering, Taiyuan University of Science and Technology, Taiyuan 030024, China. E-mail: zhangxinbox@126.com

Key words: agricultural engineering vehicles; cab; nonlinear damping; multi-objective optimization.

Conflict of interest: the authors declare no potential conflict of interest.

Funding: this research was supported by the National Natural Science Foundation of China (No. 52272401) and the Basic Research Project of Shanxi Province (No. 202203021211185).

Availability of data and material: the data used to support the findings of this study are available from the corresponding author upon request.

Received: 28 December 2023.

Accepted: 21 January 2024.

©Copyright: the Author(s), 2024

Licensee PAGEPress, Italy

Journal of Agricultural Engineering 2024; LV:1592

doi:10.4081/jae.2024.1592

This work is licensed under a Creative Commons Attribution-NonCommercial 4.0 International License (CC BY-NC 4.0).

Publisher's note: all claims expressed in this article are solely those of the authors and do not necessarily represent those of their affiliated organizations, or those of the publisher, the editors and the reviewers. Any product that may be evaluated in this article or claim that may be made by its manufacturer is not guaranteed or endorsed by the publisher.

caused by the resonance of the base plate mode of the cab, which was close to the engine excitation frequency. They focused on the purpose of vibration reduction by optimizing the design of the cab structure to avoid the resonance. Sun and Zhang (2012) established a 6-degree-of-freedom model for the cab isolation system to improve the ride comfortability of agricultural engineering vehicles. An optimization model with stiffness values as design variables was developed with the center of the cab as the optimization target. The rationality of the established optimization model was verified by establishing a finite element model of the cab and conducting modal analysis.

The direct input of the models in these studies were not the actual excitation of the cab under different conditions. That is, ignore the diversity of cab vibration sources. Therefore, the model it built may lead to relatively poor accuracy of the damping characteristics results of the cab vibration reduction system. Through test methods, this article evaluates and analyzes the damping characteristics of the cab vibration reduction system. The random vibration excitation of the cab vibration reduction system model is directly derived from the vehicle frame vibration signals obtained from the test of multiple conditions. And the model and parameter values of the suspension and seats are also obtained through the tests. Therefore, the model built can more accurately evaluate the damping characteristics of the cab.

This article takes the vibration reduction system of a certain type of agricultural loader cab as its research object. Firstly, the vibration data of specific sites of the agricultural loader cab system are obtained through vehicle tests under different conditions, including

static condition, working condition, and driving condition. Then, the non-linear damping system model of the cab-seat-human body is established with the frame vibration signal as the input. Finally, to solve the problems of excessive cab vibration and poor driving comfortability, multi-objective genetic algorithm optimization is performed with the RMS values of vertical accelerations of the cab and seat as the objectives. The test proves that the research provides a reliable and effective method for solving the problem of severe vibration in agricultural engineering vehicle cabs.

Materials and Methods

Testing equipment

The test instruments include the uT3704FRS-ICP data acquisition instrument, and the frequency range of vibration signal data acquisition is 5.12 Hz~102.4 kHz. During the experimental testing, the vibration signal data acquisition frequency was selected as 512 Hz. There are six piezoelectric IEPE acceleration sensors and six magnetic mounts. The model of the sensor and the mount is YD-37AD, and the sensitivity of the sensor is 0.504, 0.494, 0.489, 0.484, 0.478, 0.477 mv/ms^{-2} , respectively.

Test conditions and measuring point arrangement

The test circumstance is an area of wasteland, and the weather is no wind. The agricultural loader is not loaded (Figure 1A).

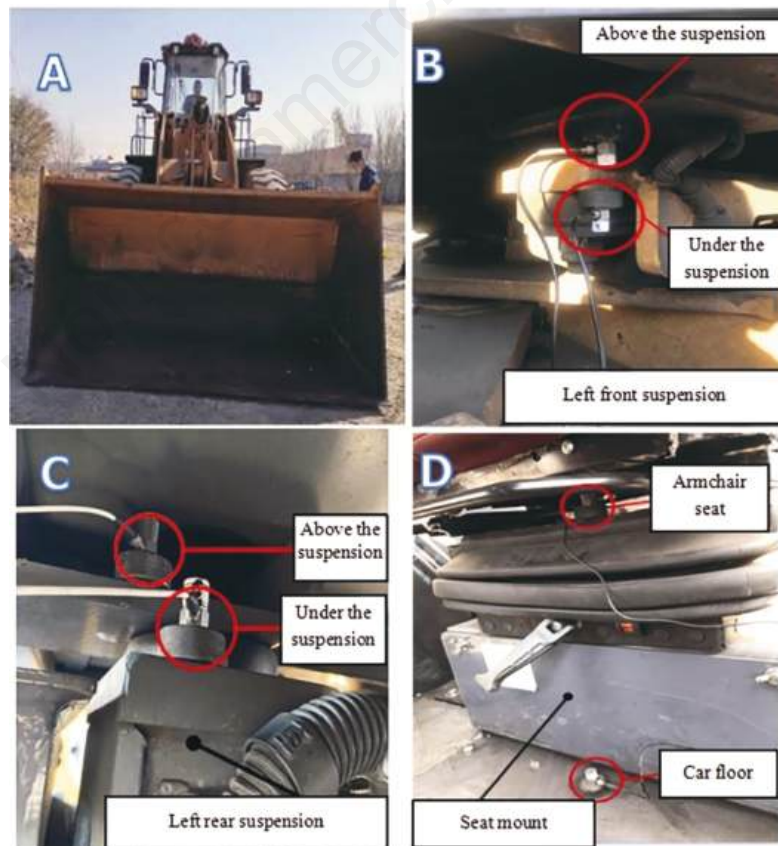


Figure 1. A) Tested vehicle. B) Seat and cab floor measuring points. C) Measured point of left front suspension of cab. D) Measured point of left rear suspension of cab.

According to the standard of GB/T4970-2009, the driver weight was selected the 50th percentile, an average weight of 65 ± 5 kg, for the experiment. The tested agricultural loader has two forward gears and one backward gear. During the driving condition, the gear selection of the loader is two, the speed is 25 km/h, and the surface of the test site comprises four types: flat cement pavement (travel straight), dirt road (travel straight), dirt road with curve (travel curve), and soil slope (travel straight uphill and downhill). During the working condition, the gear selection is one, the speed is not more than 11 km/h, and the “V” type working method is used to deal with the open-air earth mound. The vibration accelerations in the vertical direction were tested for the passive end (chassis), active end (cab bracket side), cab floor, and seat, respectively. The specific test conditions include static condition, working condition, and driving condition. The static condition includes the following different engine speeds: 800, 1000, 1300, 1400, 1500, 1800, and 2200 r/min. The agricultural loader used in this test has four cab suspensions, and sensors are installed above and below the left front and left rear cab suspensions, respectively. The Figure 1B is the left front test point of cab suspension, and the Figure 1C is the left rear test point of cab suspension. In order to avoid errors, the above and below sensors of the cab suspension should be installed on the same gravity axis. The Figure 1D is the seat and cab floor test point.

Mechanical test of seat and cab suspension

The static mechanical test of the agricultural loader seat is carried out. Different weight of testers is selected to sit and record the displacement of the seat. In order to obtain the specific parameters of the agricultural loader of cab suspension, the dynamic mechanical test of the cab suspensions is performed, and the test standard is performed according to the Japanese national standard JISK6385.

Nonlinear system modeling of cab-seat-human body

Taking an agricultural loader cab as the research object, a nonlinear damping system model of cab-seat-human body is established (Figure 2). The input is derived from the test frame vibration signal and then transmitted to the cab floor, seats, and human body through the four cab suspensions at the bottom of the cab. The main parameters of the damping system model are shown in Table 1. In the model, z_r , z_s , and z_b are the vertical displacement of the human body, seat, and cab; θ and f are the pitch angle and roll angle, respectively; $q_i(t)$ is the measured vibration signal of the suspension; f_i and c_i are the elastic force and damping coefficient of the cab suspension, respectively. Subscript $i = 1, 2, 3, 4$ represents left front, right front, right rear, left rear; f_s and c_s are the elastic force and damping coefficient of seat mount, respectively. The z_i ($i=1\sim 4$) is the vertical displacement of the above point of the cab suspension.

The relationship between z_i and z_b is as follows:

$$\begin{cases} z_1 = z_b - l_f\theta + h_r\phi \\ z_2 = z_b - l_f\theta - h_l\phi \\ z_3 = z_b + l_r\theta - b_l\phi \\ z_4 = z_b + l_r\theta + b_r\phi \end{cases} \quad (1)$$

The elastic force model of the cab suspension and seat is as follows:

$$f_i = k_{i1}(z_i - q_i(t)) + k_{i2}(z_i - q_i(t))^3 \quad (2)$$

The vertical motion equation of human body:

$$f_s = k_{s1}(z_s - z_b) + k_{s2}(z_s - z_b)^3 \quad (3)$$

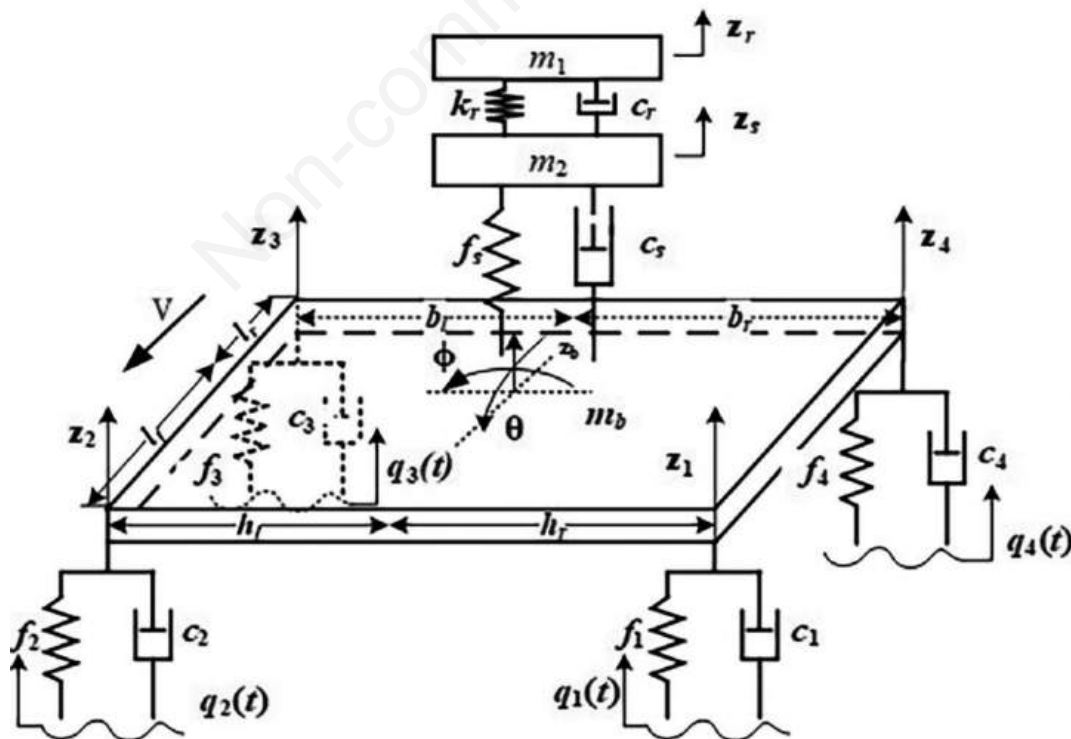


Figure 2. Nonlinear vibration model of cab-seat-human boy.

The vertical motion equation of seat:

$$m_1 \ddot{z}_r + c_r(\dot{z}_r - \dot{z}_s) + k_r(z_r - z_s) = 0 \quad (4)$$

The vertical motion equation of the body center of mass:

$$m_2 \ddot{z}_s + f_s + c_s(\dot{z}_s - \dot{z}_b) - k_r(z_r - z_s) - c_r(\dot{z}_r - \dot{z}_s) = 0 \quad (5)$$

The pitch motion equation of the body center of mass:

$$m_b \ddot{\theta} + c_1(\dot{\theta}_1 - \dot{\theta}_1(t)) + f_1 + c_2(\dot{\theta}_2 - \dot{\theta}_2(t)) + f_2 + c_3(\dot{\theta}_3 - \dot{\theta}_3(t)) + f_3 + c_4(\dot{\theta}_4 - \dot{\theta}_4(t)) + f_4 - c_5(\dot{z}_s - \dot{z}_b) - f_5 = 0 \quad (6)$$

The roll motion equation of the body center of mass:

$$I_p \ddot{\theta} - I_r[c_1(\dot{\theta}_1 - \dot{\theta}_1(t)) + f_1 + c_2(\dot{\theta}_2 - \dot{\theta}_2(t)) + f_2] + I_r[c_3(\dot{\theta}_3 - \dot{\theta}_3(t)) + f_3 + c_4(\dot{\theta}_4 - \dot{\theta}_4(t)) + f_4] = 0 \quad (7)$$

According to the theory of random vibration, a system with four inputs and five outputs is established, where $X_i(\omega)$ and $Y_i(\omega)$ are the Fourier transforms of $X_i(t)$ and $Y_i(t)$, respectively.

$X_s(t)$ is the s th input displacement, and $Y_i(t)$ is the i th output displacement. $H_{si}(\omega)$ is the frequency response function between the s th input and the i th output, and ω is the circular frequency. Through the Fourier transform, the input and output are rewritten into matrix form:

$$I_p \ddot{\theta} + h_r[c_1(\dot{\theta}_1 - \dot{\theta}_1(t)) + f_1] - h_l[c_2(\dot{\theta}_2 - \dot{\theta}_2(t)) + f_2] - h_l[c_3(\dot{\theta}_3 - \dot{\theta}_3(t)) + f_3] + b_r[c_4(\dot{\theta}_4 - \dot{\theta}_4(t)) + f_4] = 0 \quad (8)$$

$$\mathbf{X}(\omega) = [X_1(\omega) \quad \dots \quad X_4(\omega)]^T \quad (9)$$

$$\mathbf{Y}(\omega) = [Y_1(\omega) \quad \dots \quad Y_5(\omega)]^T \quad (10)$$

The frequency response matrix of the system is

$$\mathbf{H}(\omega) = \begin{bmatrix} H_{11}(\omega) & H_{12}(\omega) & H_{13}(\omega) & H_{14}(\omega) \\ H_{21}(\omega) & H_{22}(\omega) & H_{23}(\omega) & H_{24}(\omega) \\ \vdots & \vdots & \vdots & \vdots \\ H_{51}(\omega) & H_{52}(\omega) & H_{53}(\omega) & H_{54}(\omega) \end{bmatrix}$$

Suppose that the input power spectral matrix $S_X(\omega)$ of the cab-seat-human nonlinear damping system model is a 4×5 order input power spectral matrix composed of 4 input autospectra and 5 output cross-spectra:

$$\mathbf{S}_X(\omega) = \begin{bmatrix} S_{X_1X_1}(\omega) & S_{X_1X_2}(\omega) & \dots & S_{X_1X_5}(\omega) \\ S_{X_2X_1}(\omega) & S_{X_2X_2}(\omega) & \dots & S_{X_2X_5}(\omega) \\ S_{X_3X_1}(\omega) & S_{X_3X_2}(\omega) & \dots & S_{X_3X_5}(\omega) \\ S_{X_4X_1}(\omega) & S_{X_4X_2}(\omega) & \dots & S_{X_4X_5}(\omega) \end{bmatrix}$$

The 5×5 order output power spectrum matrix composed of the auto-spectrum and cross-spectrum of 5 outputs is

$$\mathbf{S}_Y(\omega) = \begin{bmatrix} S_{Y_1Y_1}(\omega) & S_{Y_1Y_2}(\omega) & \dots & S_{Y_1Y_5}(\omega) \\ S_{Y_2Y_1}(\omega) & S_{Y_2Y_2}(\omega) & \dots & S_{Y_2Y_5}(\omega) \\ \vdots & \vdots & \vdots & \vdots \\ S_{Y_5Y_1}(\omega) & S_{Y_5Y_2}(\omega) & \dots & S_{Y_5Y_5}(\omega) \end{bmatrix}$$

The relationship between the output power spectrum $S_Y(\omega)$ and the input power spectrum is

$$\mathbf{S}_Y(\omega) = \mathbf{H}^*(\omega) \mathbf{S}_X(\omega) \mathbf{H}^T(\omega) \quad (11)$$

where $H^*(\omega)$ is the conjugate matrix of $H(\omega)$.

According to random vibration theory. The four input of the nonlinear damping system model of cab-seat-human body are independent of each other. The corresponding excitation and spectrum are $X_{ii}(t)$ and $S_{ii}(t)$ ($i=1\sim 4$), respectively. The output power spectral density function of the seat $S_{zz}(f)$ can be expressed as

Table 1. Model parameters.

Parameter	Numerical value
Body mass m_1 /kg	65
Seat quality m_2 /kg	30
Cab quality m_b /kg	800
Human body equivalent stiffness k_r /(N/mm)	8.228
Human equivalent damping c_r /(N·s/mm)	0.152
Linear stiffness of seat mount k_{s1} /(N/mm)	10.18
Nonlinear stiffness of seat mount k_{s2} /(N/mm ³)	0.001568
Equivalent damping coefficient of seat mount c_s /(N·s/mm)	0.800
Left / right linear stiffness of front cab suspension k_{11}/k_{21} /(N/mm)	457.6
Nonlinear stiffness of left / right front cab suspension k_{12}/k_{22} /(N/mm ³)	20.34
Equivalent damping of left / right front cab suspension c_1/c_2 /(N·s/mm)	16.5
Linear stiffness of right / left rear cab suspension k_{31}/k_{41} /(N/mm)	454
Nonlinear stiffness of right / left rear cab suspension k_{32}/k_{42} /(N/mm ³)	46.6
Equivalent damping of right / left rear cab suspension c_3/c_4 /(N·s/mm)	5.2
Distance from cab centroid to front / rear suspension l_f/l_r /(m)	0.401/0.501
Distance from cab centroid to left / right suspension h_r/h_l /(m)	0.410/0.410
Distance from seat to left / right cab suspension b_l/b_r /(m)	0.530/0.530
Roll / pitch inertia of cab I_r/I_p (kg/m ²)	860/640

$$S_{zz}(f) = H^*(f)S_{xx}(f)H^T(f) = \sum_{i=1}^4 |H(f)|^2 S_{ii}(f) \tag{12}$$

In the formula, $H(f)$ is the system transfer matrix and $S_{zz}(f)$ is the input power spectrum matrix of the five-degree-of-freedom model, which is a diagonal matrix and can be expressed as:

$$S_{xx}(f) = \begin{bmatrix} S_{11} & & & \\ & S_{22} & & \\ & & S_{33} & \\ & & & S_{44} \end{bmatrix}$$

The corresponding RMS value can be expressed as:

$$\sigma_z = \frac{1}{T} \sqrt{\int_0^T S_{zz}(f) df} \tag{13}$$

The corresponding RMS value of vertical acceleration of seat can be expressed as:

$$S_\alpha = \frac{1}{T} \sqrt{\int_0^T \ddot{Z}_s(f) df} \tag{14}$$

The corresponding RMS value of cab vertical acceleration can be expressed as:

$$C_\alpha = \frac{1}{T} \sqrt{\int_0^T \ddot{Z}_b(f) dt} \tag{15}$$

Genetic algorithm of multi-objective optimization

The genetic algorithm begins with an initial population, which uses random selection, crossover, and mutation operations to create a group of individuals better suited to the environment (Davoodi *et al.*, 2020; Kihan *et al.*, 2020; Le *et al.*, 2018). Through successive generations, these individuals continue to evolve and multiply, converging on a group of individuals that are most suitable for the environment. This process ultimately leads to a high-quality solution to the problem, as the genetic algorithm identifies the most optimal region in the search space (Dengke *et al.*, 2023; Yang *et al.*, 2019; Cheng *et al.*, 2022; Liao *et al.*, 2021). The specific steps of the algorithm are shown in Figure 3.

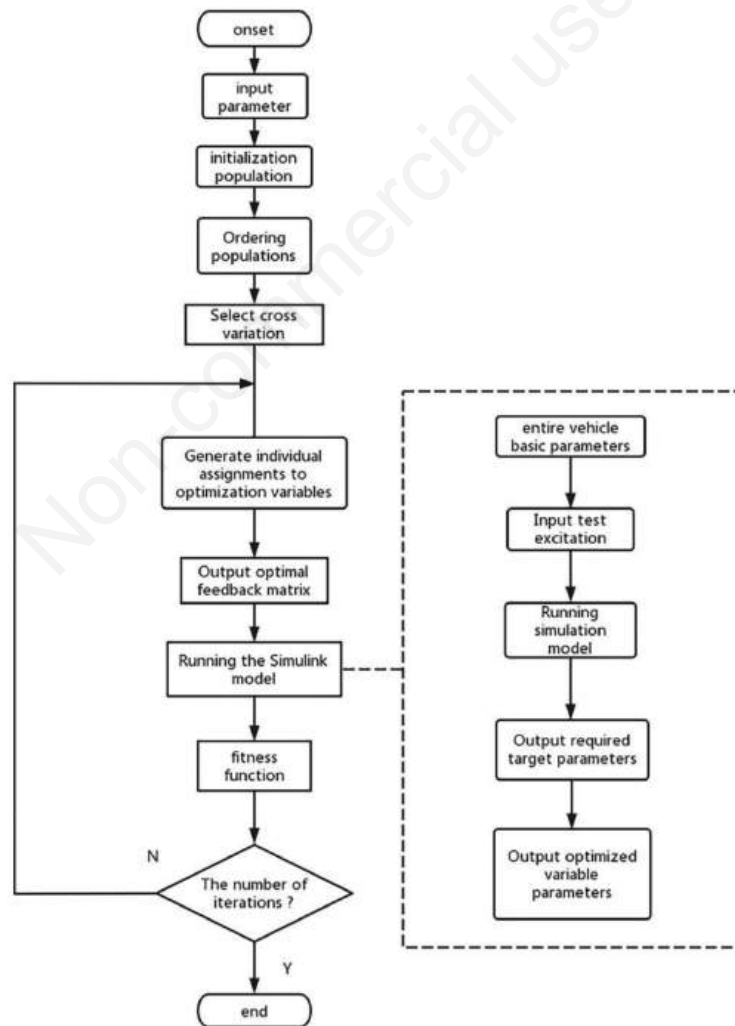


Figure 3. Specific steps of genetic algorithm.

Since the center of mass of the cab is equal to the distance between the left and right cab suspensions, the parameters of the left and right cab suspensions are the same. $A = (k_{s1}, k_{s2}, k_{s1}, k_{l1}, k_{31}, k_{32}, c_1, c_2, c_3)$ are selected as the optimization model variable, and the RMS value of the vertical acceleration of the cab and seat are set as the optimization target. The mathematical model of the multi-objective optimization design problem can be written as the following function:

$$\min_{k \in Q} \{F(A)\} = [S_\alpha(A), C_\alpha(A)] \tag{16}$$

The value ranges of the designed variable parameters are as follows:

- 30 N/mm < k_{s1} < 50 N/mm
- 1 N/mm < k_{s2} < 1 N/mm
- 400 N/mm < k_{l1}, k_{21} < 600 N/mm
- 10 N/mm < k_{12}, k_{22} < 30 N/mm
- 300 N/mm < k_{31}, k_{41} < 500 N/mm
- 30 N/mm < k_{32}, k_{42} < 50 N/mm
- 0.3 N.s/mm < c_s < 3 N.s/mm
- 12 N.s/mm < c_1, c_2 < 20 N.s/mm
- 3 N.s/mm < c_3, c_4 < 6 N.s/mm

Results

Test results of agricultural loader

The vibration transmissibility of absorber is the primary factor used to assess the performance of its vibration isolation. The vibration transmission rate of absorber is defined as:

$$T = 20|\lg(a/b)| \tag{17}$$

In the formula, a and b represent the RMS value of the cab acceleration before and after vibration reduction respectively; the bigger the T value, the better the vibration isolation effect.

The vibration of the components was tested under static condition at different engine speeds. When the engine speed is at 1400 r/min and 2200 r/min, the vibration transmission rates of suspended cab are 6.8 dB and 5.4 dB, respectively. It can be concluded that at 1400 r/min and 2200 r/min (Figure 4A), the cab suspension's ability to isolation vibration is poor; the engine is an important part of the cab vibration source and cannot be ignored. Its main vibration frequency domain is distributed between 20 and 100 Hz (Figure 4B). The driving and working conditions of the agricultural loader are tested, and the acceleration RMS values of specific

sites are shown in Table 2. After preprocessing the test data, the acceleration spectrum curves are obtained for the above and below cab suspensions under different conditions (Figure 5 A,B). The power spectral density of the seat is obtained by segmenting the spectrum (Figure 5 C,D).

Mechanical test results of seat and cab suspension

According to the static mechanical test of agricultural loader seat, the force-displacement curve of the seat is shown in Figure 6A obtained by fitting multiple sets of data. Through the dynamic mechanical test of the agricultural loader cab suspension, the specific parameters of the loader cab suspension will be obtained. First, different sinusoidal excitation loads are applied to the suspension of the cab, and then the signals fed back by the load and displacement sensor are recorded with an oscilloscope and an X-Y function meter, and the hysteresis diagram of the load-displacement curve is drawn (Figure 6B). It can be seen (Figure 6B) that the cab suspension exhibits nonlinear characteristics.

For the curves in Figure 6, the cubic fitting accuracy is higher than the quadratic fitting accuracy. Therefore, the cubic fitting equation is selected, and it is assumed that the relationship between displacement and elastic force F_K is

$$F_K = W(\Delta x) + H(\Delta x)^3 \tag{18}$$

Where W and H are the linear stiffness coefficient and the nonlinear stiffness coefficient, respectively.

The damping force F_C formula is

$$F_C = J(\Delta \dot{x}) \tag{19}$$

Where J is the damping coefficient.

After fitting calculation, The cab suspension parameters are shown in Table 1. This will provide the parameters value for the establishment of a nonlinear damping system model of cab-seat-human body.

Validation model

Taking the measured frame vibration signal as the input of the nonlinear damping system model of cab-seat-human body, the test and model curves of the vertical acceleration of cab and seat are obtained under driving and working conditions, respectively (Figure 7). It can be seen from Table 3 that the maximum error between the RMS value of test and the model of each measuring point is within 6%, indicating that the calculation accuracy of the model meets the engineering requirements. The RMS value of the seat acceleration is bigger than that of the cab, indicating that the

Table 2. Test the RMS value of vertical acceleration and vibration transmission rate.

Measuring point	Condition	Before vibration (m/s ²)	After vibration reduction (m/s ²)	Vibration transmission rate (dB)	Armchair seat
The left front measuring point Z direction	Driving	4.253	2.003	6.540	2.845
	Working	1.416	0.872	4.211	1.056
Left rear measuring point Z direction	Driving	3.825	1.258	5.816	1.632
	Working	1.215	0.458	8.474	0.752
Right front measuring point Z direction	Driving	3.956	1.859	6.560	2.362
	Working	1.185	0.482	7.791	0.625
Right rear measuring point Z direction	Driving	3.506	1.154	9.652	1.965
	Working	1.315	0.423	8.573	0.765

seat mount setting is unreasonable; under driving condition, the vertical vibration of the cab and seat is much larger than in working condition. Under working condition, the RMS value of acceleration is less than half of that in driving condition. Therefore, the driving condition is only considered in the next optimization design.

Optimization results

Based on the experience of genetic algorithm parameter setting, set the number of individuals in the multi-objective genetic algorithm population as 100, the optimal front-end individual coefficient as 0.3, the number of variables as 9, the crossover coefficient as 0.4, the maximum evolutionary generation as 20, the stop generation as 20, and the fitness function precision as 10^{-6} . The optimal multi-objective Pareto front graph is obtained through the *gplotpareto* function. Compared to other genetic algorithm parameter settings, the Pareto diagram obtained from the above settings is the best, and the calculation time is relatively short.

Taking the frame vibration signal of specific sites experimented under driving condition as input, the model parameters are substituted into the established cab-seat-human body nonlinear vibration model to optimize under driving conditions. The optimization Pareto diagram is shown in Figure 8. It can be seen from Figure 8 (Pareto diagram) that the objective function value basically consti-

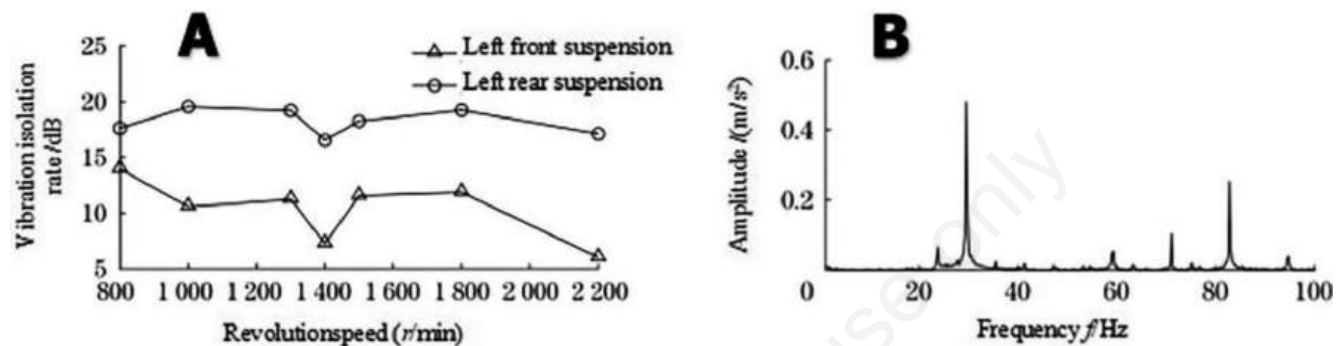


Figure 4. A) Vibration transmissibility of cab at different engine speeds under static condition. B) Seat spectrum at 1400r/min of engine speed under static condition.

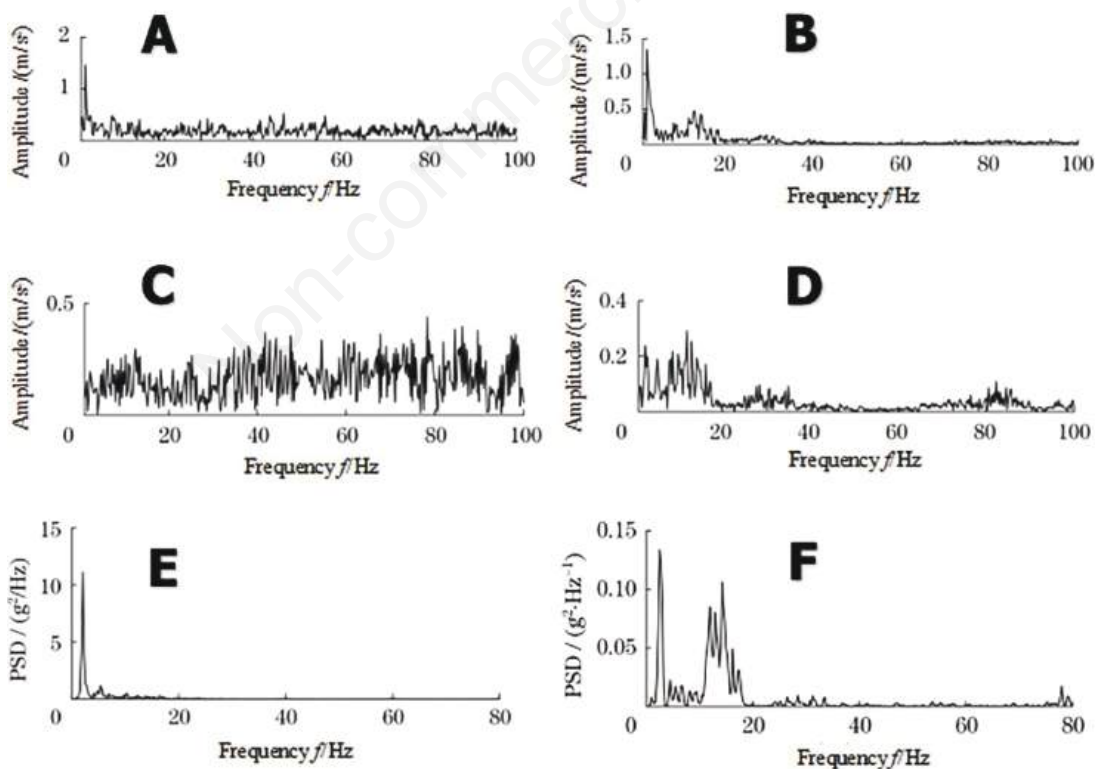


Figure 5. A) Vertical acceleration spectrum diagram of left front measuring point under driving condition (Before vibration reduction). B) Vertical acceleration spectrum diagram of left front measuring point under driving condition (after vibration reduction). C) Vertical acceleration spectrum diagram of left front measuring point under driving condition (before vibration reduction). D) Vertical acceleration spectrum diagram of left front measuring point under driving condition (after vibration reduction). E) Power spectral density of vertical acceleration of seat under driving condition. F) Power spectral density of vertical acceleration of seat under driving condition.

tutes a smooth curve, and each solution is evenly distributed, indicating that the Pareto diagram contains most of the optimal solutions, with Global optimization and strong applicability. In engineering applications, the driver's comfortability is particularly important, so the weight of the RMS value of the seat's vertical acceleration should be greater in the optimization results. After careful consideration, the weight coefficients of the seat and the cab are selected to be 0.9 and 0.1, respectively. The corresponding multi-objective optimization results are obtained according to Figure 8, as shown in Table 4. Table 4 shows the optimization parameters of the nonlinear vibration reduction system of cab. Finality, a sensitivity analysis was conducted on the obtained results, and it was found that their sensitivity is low.

selection parameters are unreasonable. The vibration of driving condition is worse than that of working condition. It can also be seen that the seat vibration is amplified, and the power spectrum value of the vertical acceleration of the seat is big under the driving condition, which proves that the seat design is unreasonable (Figure 5 E,F). In addition, because the vibration source of the cab mainly includes the engine and working device under the working conditions, it can be seen from the test results that the working device cannot be neglected as the vibration source of the cab. According to the standard ISO2631-1, when the peak coefficient of the vibration waveform is less than 9, the RMS value of weighted acceleration a_w can be used to evaluate the vibration on the human body. The formula is as follows:

$$a_w = \left[\int_{0.5}^{80} w^2(f) G_a(f) df \right]^{1/2} \quad (20)$$

Where $G_a(f)$ is the power spectral density function of acceleration time history; f is the frequency; and $w(f)$ is the frequency-dependent weight function, which can be expressed as:

Discussion

From Table 2 and Figure 5, it can be seen that the vibration transmission rate of the cab suspension is between 4.211 dB and 9.652 dB under driving and working conditions, and the damping effect of the suspension is poor, which proves that the suspension

Table 3. Errors of RMS value of vertical acceleration between theoretical model and test.

Condition	RMS value of vertical acceleration	Experimental value (m/s ²)	Theoretical value (m/s ²)	Error (%)
Driving	S_a	2.899	2.845	1.86
	C_a	2.003	1.975	1.39
Working	S_a	1.123	1.056	5.97
	C_a	0.912	0.872	4.38

Table 4. The multi-objective optimization results with seat and cab weight coefficients of 0.9 and 0.1, respectively.

Armchair seat		Front suspension		Rear suspension	
$k_{s1}/$ (N/mm)	15.35	$k_{11}/$ (N/mm)	465.3	$k_{31}/$ (N/mm)	425.5
$k_{s2}/$ (N/mm ³)	0.024	$k_{12}/$ (N/mm ³)	24.28	$k_{32}/$ (N/mm ³)	45.8
$c_s/$ (N·s/mm)	0.77	$c_1/$ (N·s/mm)	15.7	$c_3/$ (N·s/mm)	4.8

Table 5. Evaluation of seat comfortability under different test conditions.

Condition		Weighed RMS acceleration a_w (m/s ²)	Human's subjective reactions
Static	800 r/min	0.035	No discomfort
	1400 r/min	0.056	Slight discomfort
	2200 r/min	0.086	Less comfortable
Driving	25 km/h	2.485	Uncomfortable
Working	"V" type working method	0.925	Very uncomfortable

Table 6. Experiment to verify the optimization effect.

RMS (m/s ²)	Driving condition		Working condition	
	S_a	C_a	S_a	C_a
Experimental value before optimization	2.899	2.003	1.123	0.912
Theoretical value after optimization	1.368	1.962	0.583	0.731
Experimental value after optimization	1.396	1.953	0.621	0.775
Improvement rate	51.84%	2.49%	44.70%	15.85%

$$w(f) = \begin{cases} 0.5 & (0.5\text{Hz} < f < 2\text{Hz}) \\ f/4 & (2.0\text{Hz} < f < 4.0\text{Hz}) \\ 1.0 & (4.0\text{Hz} < f < 12.5\text{Hz}) \\ 12.5/f & (12.5\text{Hz} < f < 80\text{Hz}) \end{cases}$$

The vibration response of tested seat can be measured under different conditions. By substituting the test response data into Formula (20), the RMS value of weighted acceleration can be calculated, and according to the standard ISO2631 of comfortability of agricultural loader seat, the driver’s comfortability is evaluated.

The comfortability of the agricultural loader seat in different conditions by Formula (19). As shown in Table 5. It is found that the RMS value of weighted vertical acceleration of the seat is less than 0.315 m/s², in which value the human body’s subjective feeling is comfortable, in different engine speeds under the static condition. Under driving condition, the RMS value of the vertically

weighted acceleration is greater than 2 m/s², in which value the human body’s subjective feeling is extremely uncomfortable. Under the working condition, the RMS value of the vertically weighted acceleration is between 0.8 and 1.6 m/s², in which value the human body’s subjective feeling is uncomfortable. In summary, the vibration isolation performance of cab suspension and seat comfortability of the agricultural loader have certain potential for improvement during driving and operation.

The vibration response before and after optimization is calculated by the theoretical model (Figure 9): under the driving condition, the RMS value of the acceleration of the optimized cab is reduced by 2.49 % compared with that before optimization, and the RMS value of seat acceleration is reduced by 51.84 %, and the seat comfortability is obviously improved (Figure 9 A,E). Under the working condition, the RMS value of acceleration of optimized cab is reduced by 15.85%, and the RMS value of acceleration of

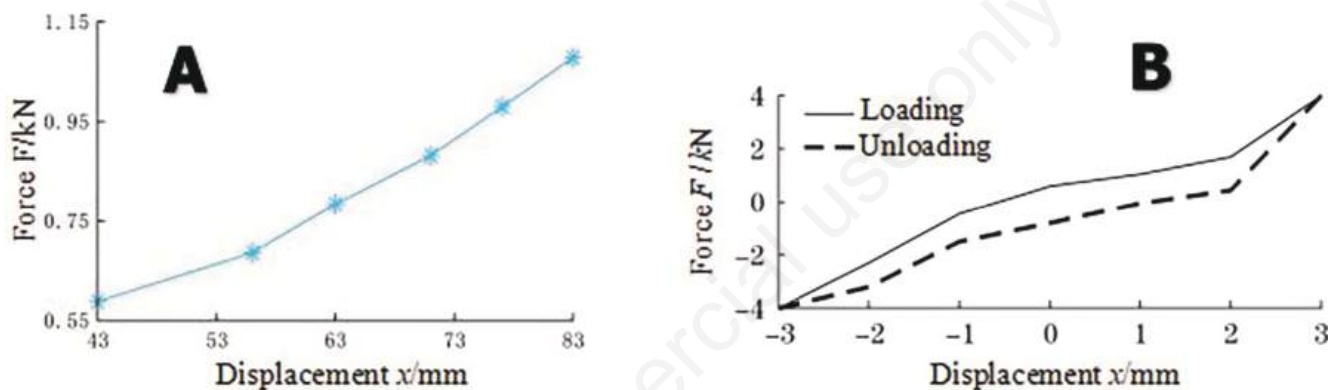


Figure 6. A) The relationship between force and displacement of seat mount. B) Load- displacement hysteresis loop of cab suspension.

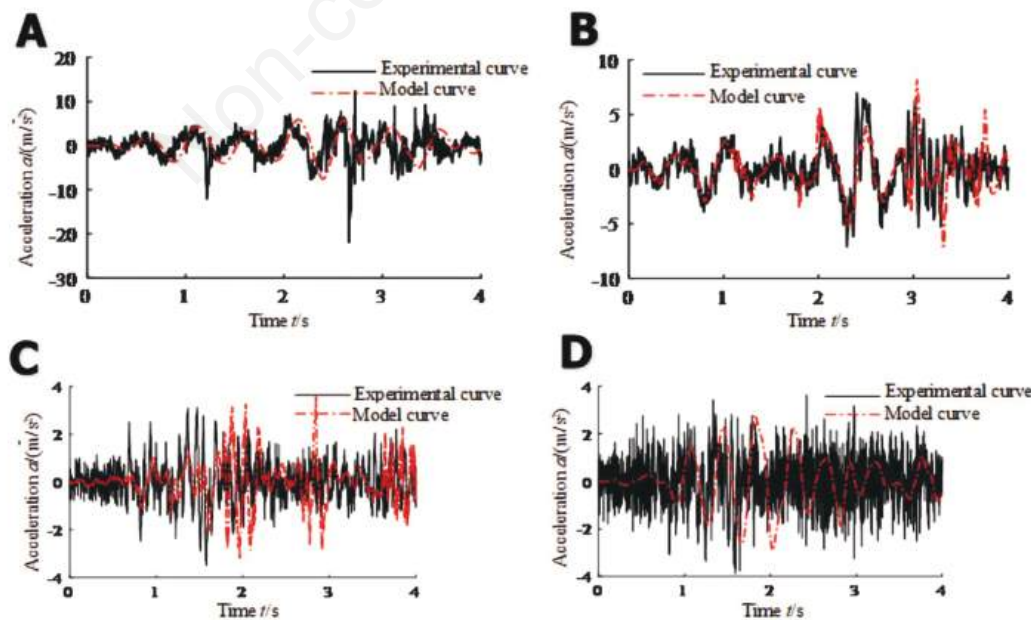


Figure 7. A) Vertical acceleration of seat under driving condition. B) Vertical acceleration of cab under driving condition. C) Vertical acceleration of cab under working condition. D) Vertical acceleration of seat under working condition.

seat is reduced by 44.70%, and the seat comfort is improved (Figure 9 C,F). Under driving and working conditions, the peak value of the seat acceleration frequency domain curve is obviously reduced after optimization (Figure 9 B,D). After optimization, the vehicle is experimented at the same materials and methods, the

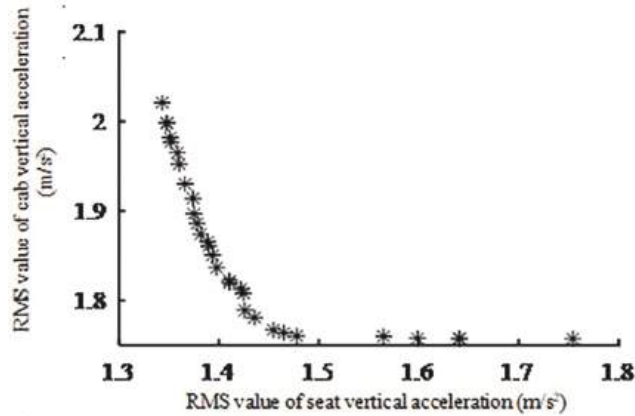


Figure 8. Pareto diagram under driving condition.

experiment results of the improved vehicle are shown in Figure 10. It can be seen from Table 6 that the error between the improved theoretical and experimental value is 3.28%, after improvement, and the improvement rate of RMS value of seat and cab acceleration is 51.84% and 2.49% under driving condition, respectively. At the same time, the improvement rate of RMS value of seat and cab acceleration is 44.70% and 15.85% under working condition, respectively. The vibration reduction system of optimized cab has been improved.

Conclusions

The test results show that the vibration transmission rate of the cab before optimization ranged from 4.211 to 9.652 dB. The vibration of the cab under driving conditions is significantly greater than that under working and stationary conditions, and the RMS value of the seat acceleration is more than the corresponding value of the cab. By using the measured frame vibration signal as the input, a nonlinear vibration reduction system model was established for cab-seat-human body of the agricultural loader. Comparing the RMS values of the vertical acceleration of the theoretical model and vehicle test, the error does not exceed 6%, indi-

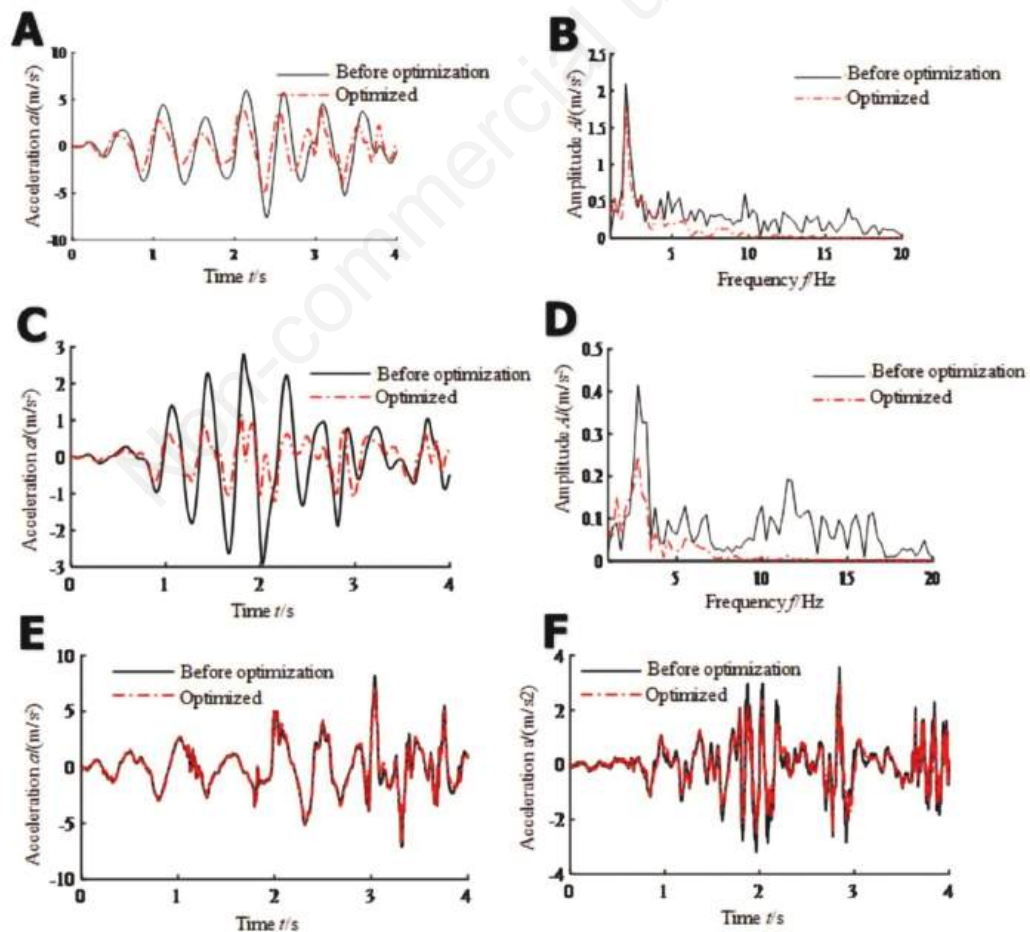


Figure 9. A) Vertical acceleration of seat under driving condition. B) Frequency domain curves of seat vertical acceleration under driving condition. C) Vertical acceleration of seat under working condition. D) Frequency domain curves of seat vertical acceleration under working condition. E) Vertical acceleration of cab under driving condition. F) Vertical acceleration of cab under working condition.

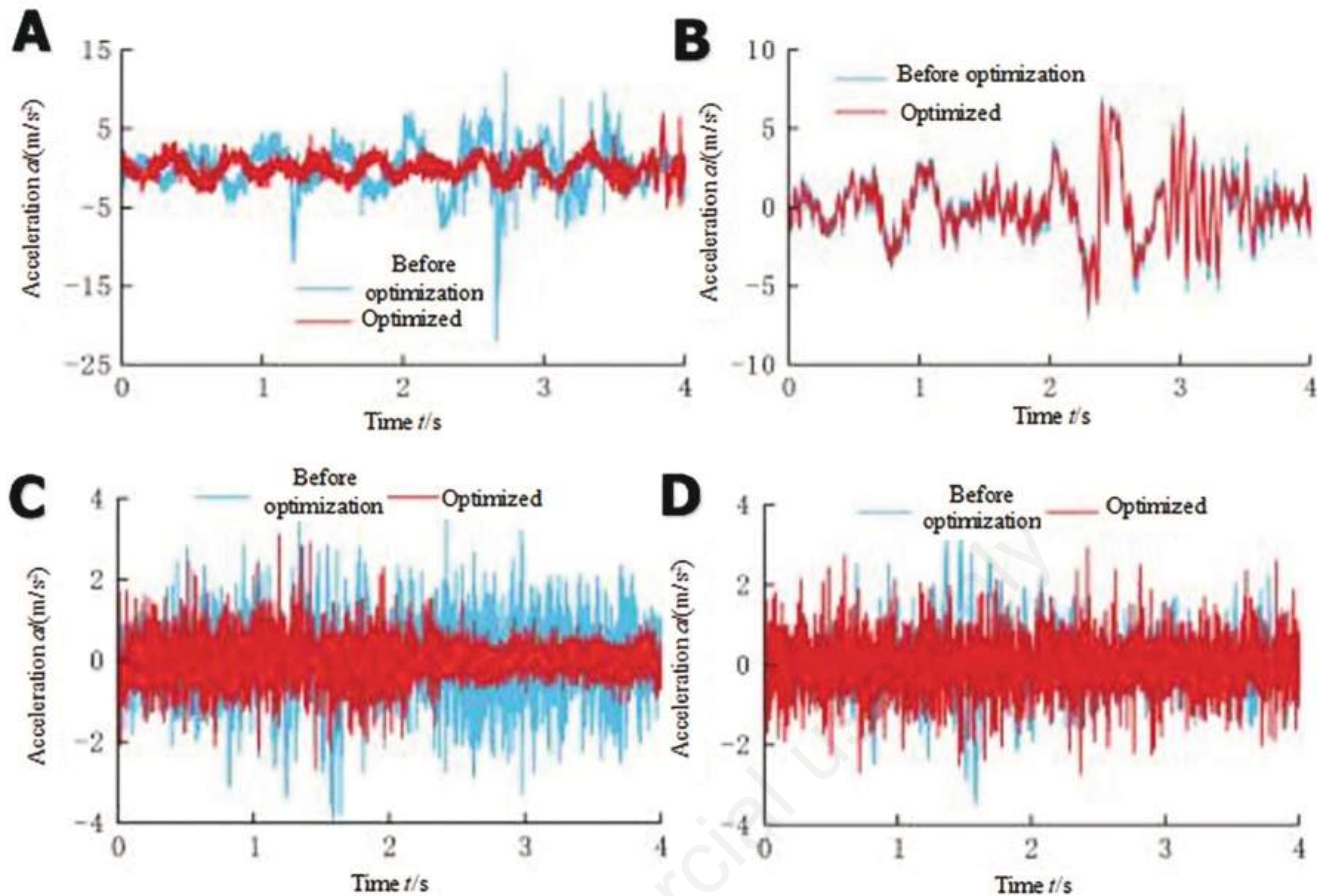


Figure 10. A) Vertical acceleration of seat under driving condition. B) Vertical acceleration of cab under driving condition. C) Vertical acceleration of seat under working condition. D) Vertical acceleration of cab under working condition.

cating that the model's accuracy meets the requirement. This model can serve as a theoretical basis for the subsequent research on vibration reduction systems for the driver's compartment.

The experiment results of the vehicle show that, by contrast with pre and post optimization, the RMS value of the vertical seat acceleration decreases by 48%~52%, while the RMS value of the vertical acceleration of cab decreases by 2%~16%. The optimization improves the vibration reduction performance of the cab and the comfortability of the seat.

References

- Cheng, L., Wen, H.S., Ni, X.Y., Zhuang, C., Zhang, W.J., Huang, H.B. 2022. Optimization study on the comfort of human-seat coupling system in the cab of construction machinery. *Machines* 11:30.
- Davoodi E., Safarpour, P., Pourgholi, M., Khazaei, M. 2020. Design and evaluation of vibration reducing seat suspension based on negative stiffness structure. *J. Mech. Eng. Sci.* 234:4171- 4189.
- Debeleac, C. 2021. Dynamic modeling and simulation of working regime of the hydraulic driven of auger bucket for loader using Matlab/SimHydraulics. *Hidraulica* 4:7-16.
- Dengke, N., Renqiang, J., Vanliem, N., Zhang, J.R. 2023. Enhancing the ride comfort of off-road vibratory rollers with seat suspension using optimal quasi-zero stiffness. *J. Mech. Eng. Sci.* 237:482-496.
- Jamali, A., Shams, H., Fasihozaman, M. 2014. Pareto multi-objective optimum design of vehicle-suspension system under random road excitations. *P. I. Mech. Eng. K-J. Mul.* 228:282-293.
- Junji, Y., Koki, T., Ryo, M., Rie, N., Ken, F. 2017. Factor analysis of cab vibration of a construction machine model using mode shape correlation between operational principal component mode and vibration mode. *I. Noise Control. Eng.* 255:1121-1129.
- Kihan, K., Minsik, S., Hansu, K., Hee, L.T., Jongseok, L., Seungjae, M. 2020. Multi-objective optimisation of hydro-pneumatic suspension with gas-oil emulsion for heavy-duty vehicles. *Vehicle. Syst. Dyn.* 58:1146-1165.
- Le, V.Q., Nguyen, K.T. 2018. Optimal design parameters of cab's isolation system for vibratory roller using a multi-objective genetic algorithm. *Appl. Mech. Mater.* 4579:105-112.
- Li, P.Q., Wang, Y.W., Cheng, W.T. 2021. Simulation analysis of cab mounting system of flat-head truck. *J. Phys. Conf. Ser.* 1885:1-7.
- Li, X.F., Lv, W.D., Zhang, W., Zhao, H.Y. 2017. Research on

- dynamic behaviors of wheel loaders with different layout of hydropneumatic suspension. *J. Vibroeng.* 19:5388-5404.
- Liao, X., Wang, H. 2021. Modeling and dynamic analysis of hydraulic damping rubber mount for cab under larger amplitude excitation. *J. Vibroeng.* 23:542-558.
- Liu, C.J., Chen, Z.L., Lv, X.L., Shang, Q. 2020. Research on vibration reduction optimization of a construction machinery cab. *Mech. Sci. Technol.* 39:682-687.
- Lin, J.W., Lin, Z.F., Ma, L., Xu, T.S., Chen, D., Zhang, J. 2019. Analysis and optimization of coupled vibration between substructures of a multi-axle vehicle. *J. Vib. Control.* 25:1031-1043.
- Nguyen, V., Jiao, R.Q., Le, V., Wang, P.L. 2020. Study to control the cab shaking of vibratory rollers using the horizontal auxiliary damping mount. *Math. Probl. Eng.* 6:57-65.
- Palumbo, A., Polito, T., Marulo, F. 2021. Experimental modal analysis and vibro-acoustic testing at leonardo laboratories. *Mater Today-Proce.* 34:24-30.
- Stan, C., Iozsa, D., Oprea, R.A. 2015. The influence of the chassis' parameters on the truck vibrations transmissibility. *Appl. Mech. Mater.* 4239:809-810.
- Sun, X.J., Zhang, J.R. 2012. Optimization of low-frequency vibration isolation for cab ride comfort of construction machineries. *J. Agric. Eng-Italy.* 28:44-52.
- Sun, Z.E., Liu, S., Xue, K. 2020. Vibration test research and analysis of a certain type of engineering machinery cab. *Noise. Vib. control.* 40:187-192.
- Tao, W., Liu, Z.Q., Chen, S.B., G Y. 2020. Suspension damping design of wheel loader cab based on fuzzy control. *Road Traff. Technol.* 37:118-129.
- Yang, F.X., Zhao, L.L., Yu, Y.W., Zhou, C.C. 2019. Matching, stability, and vibration analysis of nonlinear suspension system for truck cabs. *Shock. Vib.* 2019:1-10.
- Zhao, L.L., Guo, J., Yu, Y.W., Li, X.H., Zhou, C. 2020. Simulation of nonlinear vibration responses of cab system subject to suspension damper complete failure for trucks. *Int. J. Model. Simul. Sci.* 11:13-13.
- Zeng, Q.Q. 2011. Multi-body dynamics analysis of the structural system of 80-wheel loader. Degree Diss., Jilin University, China.